Transactions, SMiRT-24
BEXCO, Busan, Korea - August 20-25, 2017
Division II

EVALUATION OF CREEP CRACK GROWTH RATE FOR GRADE 91 Weldment AT 550°C

Woo-Gon Kim[1], Jae-Young Park[2], Eung-Seon Kim [3], and Min-Hwan Kim[4]

[1] Principal Researcher, Advanced Materials Development Team, Korea Atomic Energy Research Institute, Korea
[2] Post Doctor, Nuclear Materials Research Div., Korea Atomic Energy Research Institute, Korea
[3] Principal Researcher, HTGR Development Div. Korea Atomic Energy Research Institute, Korea
[4] Principal Researcher, HTGR Development Div. Korea Atomic Energy Research Institute, Korea

ABSTRACT

The purpose of this study is to quantitatively evaluate a creep crack growth rate (CCGR) for the base metal (BM), weld metal (WM), and heat affected zone (HAZ) of Gr. 91 weldment, which was prepared by a shield metal arc weld (SMAW) method. A series of tensile, creep, creep crack growth (CCG) tests were performed for the BM, WM, and HAZ at the identical temperature of 550°C. The CCG data was obtained under different applied loads using a direct current potential drop (DVPD). The CCGR equations for the BM, WM, and heat HAZ were obtained in terms of time-dependent C^* fracture parameter, and each CCGR law was constructed and compared. Results showed that the CCGRs of the WM and HAZ were faster than that of the BM, and the CCGR line of the HAZ was transitionally changed between those of the WM and BM. Currently elevated temperature design (ETD) code in French, RCC-MRx was found to be more conservative in the CCGR than the KAERI data obtained in the present investigation.

INTRODUCTION

Modified 9Cr-1Mo steel (ASME grade 9Cr-1Mo, hereafter Gr.91) is regarded as a promising candidate for structural materials of Generation-IV reactor types such as steam generators, intermediate heat exchangers and hot pipes in sodium-cooled fast reactors (SFR), and particularly pressure vessels in very high temperature reactors (VHTR)(Kim et al.(2014) and Choudhary et al. (1999)). Their structural components are designed to last for up to 60 years at elevated temperatures and will be often subjected to non-uniform stress and temperature distribution during a long service. These conditions may generate localized creep damage and propagate the cracks and ultimately may cause a fracture. A significant portion of their lives will be spent during crack propagation (Nikbin et al. (1986), Kim et al. (2011), and Takahasi et al. (2005)). It is therefore necessary to evaluate creep crack growth (CCG) behavior during creep loading for design and safety assessment of the components, especially for Type IV cracking of a heat affected zone (HAZ) in weldments of high-Cr ferrite and martensite (FM) steels. It is known that 9Cr or 12Cr steel tends to fail with Type IV cracking at welded joints, resulting in shorter plant life than expected. To prevent such unexpected failures, an accurate residual life assessment method for the welded joints is required.
Generally, welded joints are considered as the composite structure of different materials consists of base metal (BM), weld metal (WM), and HAZ. Since the inhomogeneity among those materials affects the state of stress field or strain rate field near the weld fusion line and near the BM/HAZ interface, it is not easy to estimate the crack propagation behavior at the welded joint. Also, it is concerning that the difference in creep deformation properties among the BM, WM, and HAZ may bring about a difficulty in the crack assessment process (Tabuchi et al. (2001), Sugiura et al. (2007), and Yamamoto et al. (2010)).

Therefore, it is necessary to clarify the creep crack growth (or creep crack propagation) laws through experimental CCG tests for the weld joint of Gr. 91 steel.
This paper is to comparatively investigate the CCGRs for the BM, WM, and HAZ in the weldment of Gr. 91, which is prepared using a shielded metal arc weld (SMAW) process. The CCGR laws for the BM, WM, and HAZ are constructed in terms of a C^* fracture parameter, and they are compared and discussed using the RCC-MRx data of currently elevated temperature design (ETD) code in French.

EXPERIMENTAL PROCEDURES

The Gr. 91 steel used in this study was a commercial type hot rolled plate 32mm in thickness. Heat treatment conditions were normalized and tempered (N+T) at 1050°C /1mim per mm and 770°C/3mim per mm. The groove shape of the welding of two plates was designed as a single V-groove with 60 degrees. Welded blocks were prepared by using the shielded metal arc welding (SMAW) process. The filler metal, CM-9Cb (brand name), was manufactured by Kobe steel as AWS Class, E9016-G (3.2-4.0 mm). The post weld heat treatment was maintained for 255 min at 750°C.
In addition, to obtain the material properties for the BM, WM, and HAZ regions, a series of tensile and creep tests were performed at the identical temperature of 550°C. The HAZ specimens were cut out toward the transverse direction against the welding direction (longitudinal direction) in the welded block. The tensile specimens had a rectangular cross section of 2mm in thickness and 6.25mm in width, with a 25mm gauge length. The strain rate was conducted with $1\text{x}10^{-4}$ /s at 550°C. The creep specimens had a cylindrical shape with a 30 mm gauge length and 6 mm diameter. The HAZ specimens position the HAZ location at the centre of gauge length. Using constant-load creep machines of a dead-weight type with lever ratio of 20:1, creep tests were carried out with different stress levels at 550°C. Creep strain data with elapsed times were taken automatically by a PC through a high precision LVDT. The steady state creep rate was measured from the secondary creep region of experimental creep curves. The experimental procedures for the creep tests followed the recommendations of the ASTM standard E139 (ASTM, (2013)). From these tensile and creep tests, the material constants of D, m, A, and n were obtained for the BM, WM, and HAZ samples.
The CCG tests for the BM, WM, and HAZ samples were carried out at a constant load with different applied load levels at 550°C. Compact tension (CT) specimens had a width (W) of 25.4mm, a thickness (B) of 12.7mm, and side grooves of a 10% depth. The initial crack ratio (a/W) was about 0.5, and the pre-cracking size was 2.0mm and was machined by an electric discharge machining (EDM) technique to introduce a sharp crack tip starter for the BM, WM, and HAZ regions. In the welded joint, sharp pre-cracks for the HAZ were taken to conform to one of the HAZ locations. Load-line displacement was measured using a linear gauge assembly attached to the specimen, and the crack length was determined using a direct current potential drop (DCPD) technique, as shown in Figure 1. Crack extension data were continuously collected using a data acquisition system. All of the experimental procedures followed the recommendations of the ASTM standard E1457 (ASTM, (2013)). After the CCG testing, the CT specimens were broken open at liquid nitrogen temperature to measure the actual crack length. The actually measured final crack length (a_{mf}) was calculated from measurements made on the fracture surface at nine equally spaced points (so-called “nine points method”) using the enlarged photo of the fractured surfaces, because the individual measurements on the fracture surface vary due to crack front irregularities.
In addition, the predicted crack length (a_{p}) by DCPD technique was calculated by Johnson’s formula:

$$\frac{a_p}{W} = \frac{2}{\pi}\cos^{-1}\left[\frac{\cosh(\pi Y_o / 2W)}{\cosh\left[\frac{V}{V_o}\cosh^{-1}\left\{\frac{\cosh \pi Y_o / 2W}{\cosh \pi a_o / 2W}\right\}\right]}\right] \tag{1}$$

where, a_o = initial crack size (reference crack size for the reference voltage V_o), Y_o = the half distance between the output voltage loads, V = the output voltage, and W = the width of specimen. The a_p was compensated by the potential measurement error and became the corrected crack length a:

$$a = \frac{a_{mf} - a_o}{a_{pf} - a_o}(a_p - a_o) + a_o \tag{2}$$

where, a_{pf} is the predicted value of the final crack length. Hence, the difference values between the a_{mf} and a_{pf} were investigated whether their values were fairly included within the requirements of ASTM E1457 (ASTM, (213)), or not. Namely, the CCG data are valid for further processing if

$$0.85 \le (\Delta a_{pf} / (a_{mf} - a_o) \le 1.15 \tag{3}$$

where, the predicted crack extension, Δa_{pf}, was calculated by substrating the initial crack length, a_o, from the finally predicted crack length, a_{pf} (Dogan and Petrovski (2001)). From these procedures, the validity for the CCG tests were identified for all the tested CT specimens.

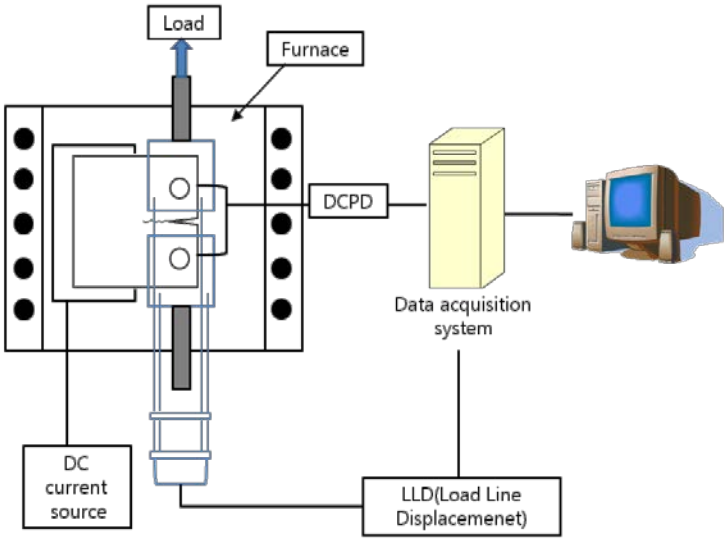

Figure 1. A schematic diagram for the CCG tests.

In the BM, the CCG tested data were obtained for seven samples with the applied load ranges of 6200N to 8000N. And in the WM, the CCG test data were obtained for six samples with the applied load ranges of 5700N to 6200N. Then in the HAZ, the CCG test data were obtained for five samples with the applied load ranges of 6600N to 7000N, respectively.

RESULTS AND DISCUSSION

Material Constants

The variations of micro-Vickers hardness for the BM, WM and HAZ regions in the welded joint were measured, as shown in Figure 2. The thickness of the HAZ region was around 3.0-5.0mm. The hardness of the WM region shows higher values than that of the BM and HAZ regions, and particularly, the hardness in the HAZ decreases transitionally between the BM and WM. This HAZ will be very weak

from cracks compared with the BM and WM, and it will initiate Type-IV crack in fine-grained zone which is located in the HAZ adjacent to the parent metal. It is known that the Type-IV cracks are parallel or offset from the fusion line.

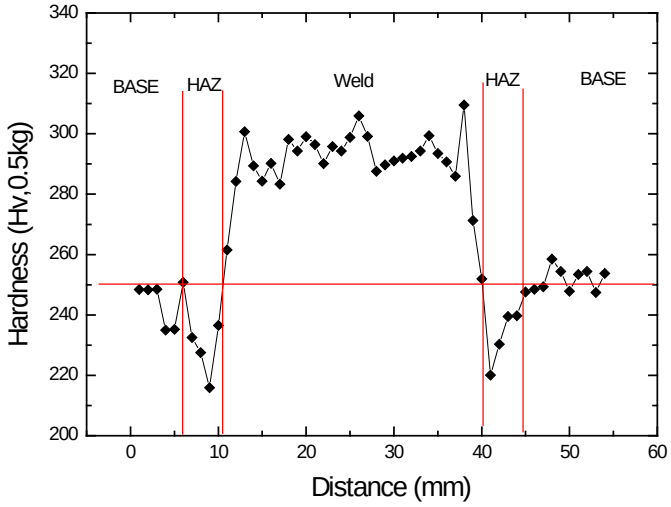

Figure 2. Vickers micro-hardness for BM, WM, and HAZ of Gr. 91 steel.

The *D* and *m* constants for the BM, WM, and HAZ were obtained from the tensile tests at 550°C. Plastic constants were obtained in terms of $\varepsilon_p = D(\sigma/\sigma_y)^m$, where ε_p = true plastic strain, σ = true stress, and σ_y = yield stress. The relationship between plastic strain and true stress followed good linearity. From this linear relation, the *D* and *m* values for the BM, WM, and HAZ could be obtained.

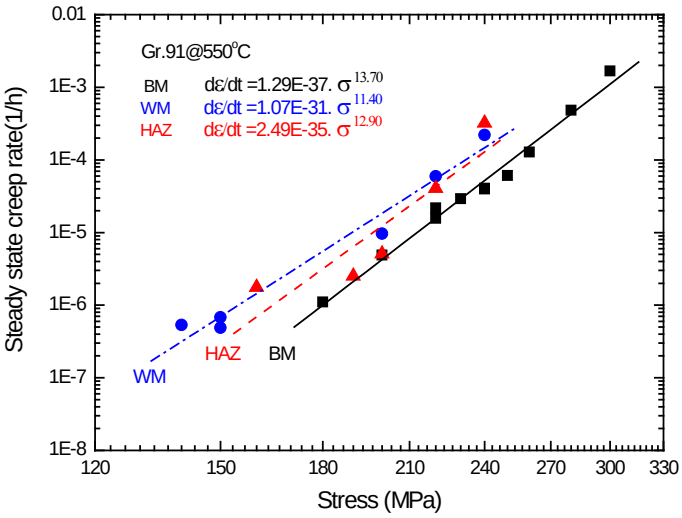

Figure 3. Comparison of the steady state creep rate for the BM, WM, and HAZ at 550°C.

In addition, the creep constants of *A* and *n* were obtained by a series of the creep tests for the BM, WM, and HAZ at 600°C. Figure 3 shows the relationships between steady state creep rate and applied stress, which followed good linearity based on Norton's power law. The WM and HAZ were higher in *A* and *n* values than the BM, and the HAZ is transitionally changed between the BM and WM. However, the HAZ is almost similar to the WM in the creep strain rate. The creep strain rates of the WM and HAZ was found to be the difference of one order approximately to the BM. It is believed that the WM and HAZ will be

significantly attributed to a faster crack propagation rate. Accordingly, through the tensile and creep tests at 550°C, the material constants of *D*, *m*, *A*, and *n* were obtained for the BM, WM, and HAZ, respectively. A summary of these material constants, which were used to calculate the C^* fracture parameter later, is given in Table 1.

Table 1. A summary of material constants obtained for the BM, WM, and HAZ at 550°C.

Material	σ_y (MPa)	$\varepsilon_p = D(\sigma/\sigma_y)^m$		$\dot{\varepsilon}_s = A\sigma^n$	
		D	*m*	*A*($MPa^{-n}h^{-1}$)	*n*
BM	338	1.23E-03	15.45	1.29E-37	13.70
WM	376	1.86E-03	13.55	1.07E-31	11.40
HAZ	321	1.76E-03	12.44	2.49E-35	12.90

Calculation of C* -parameter

The fracture mechanics parameter, C^*-integral, has been widely used to characterize the creep crack growth rate in metals undergoing a steady state creep (Saxena (1997) and Nikbin(1986)). The steady state creep rate can be written using Norton's power law:

$$\dot{\varepsilon}_{ss} = A\sigma^n \tag{4}$$

The general form between the creep crack growth rate (*da*/*dt*) and the C^* can be expressed by

$$da/dt = B[C^*]^q \tag{5}$$

where *n* is the creep exponent, and the *B* and *q* coefficients are material constants, which are generally obtained from a regression line of the CCGR data. They are related to the intercept and slope, respectively, of the *da*/*dt* vs. C^* relationship on a log-log plot. To calculate the *da*/*dt* in Eq. (5), material data obtained in Table 1 were used to calculate the C^* values. The relationship between *da*/*dt* and C^* was obtained for all samples.

In the CT specimen, the C^* value was calculated using Eq. (6), and load-line displacement rate ($\dot{V}_c$) due to creep strain was calculated by Eq. (8).

$$C^* = \frac{P\dot{V}_c}{B_N W}\eta\left(\frac{a}{W}, n\right) \tag{6}$$

$$\eta\left(\frac{a}{W}, n\right) = \frac{1}{(1-a/W)}\frac{n}{n+1}\left(\gamma - \frac{\delta}{n}\right) \tag{7}$$

$$\dot{V}_c = \dot{V} - \frac{\dot{a}B_N}{P}\left(\frac{2K^2}{E'} + (m+1)J_p\right) \tag{8}$$

where *P* = applied load, *a* = crack size, *W* = width of the specimen, $\dot{V}$ = total load-line displacement rate, B_N = net thickness of specimen, *E'*= elastic modulus for plane strain, *K* = stress intensity factor, $\dot{a}$ = crack growth rate, and *m* = stress exponent in the Ramberg-Osgood stress versus strain relationship.

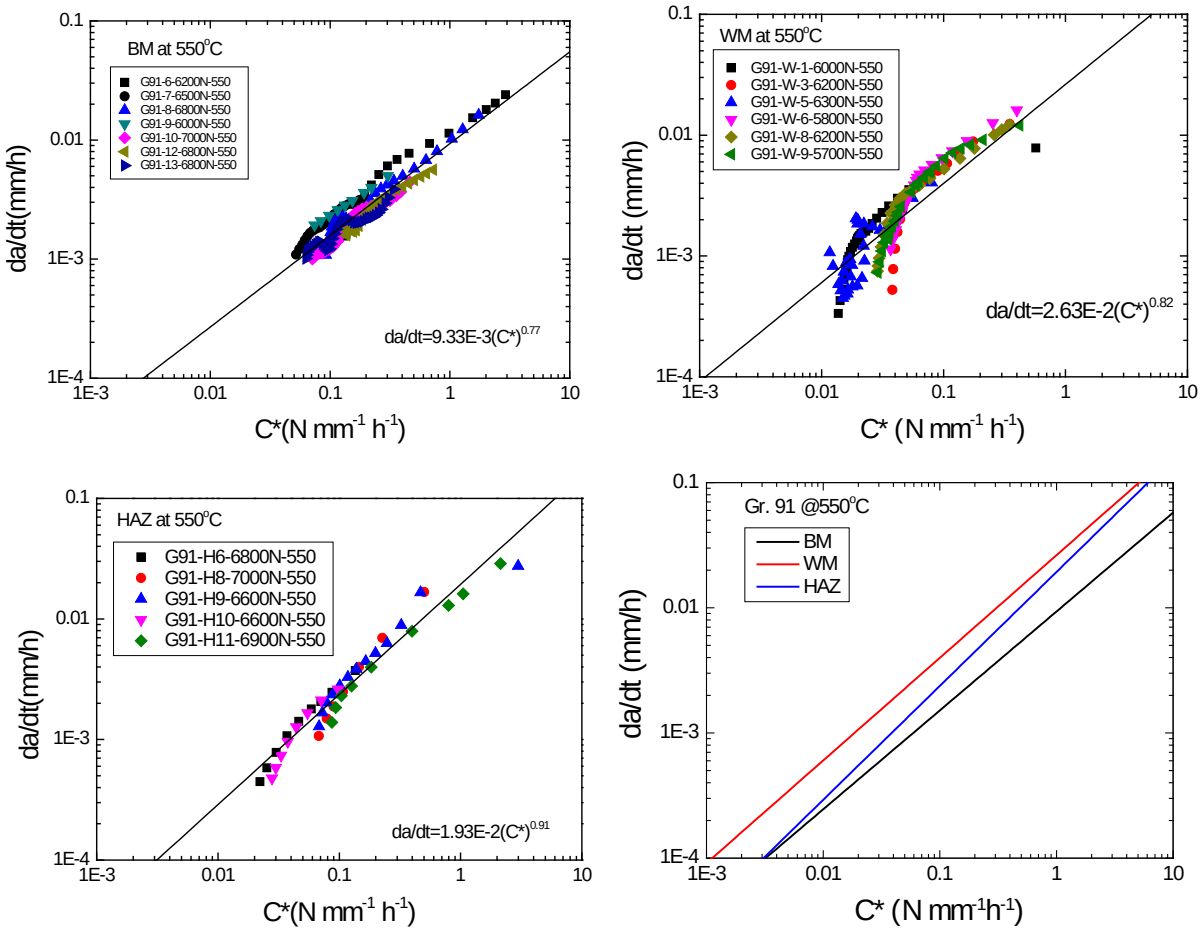

Figure 4. Plot of C^* vs. CCGR for the BM, WM, and HAZ

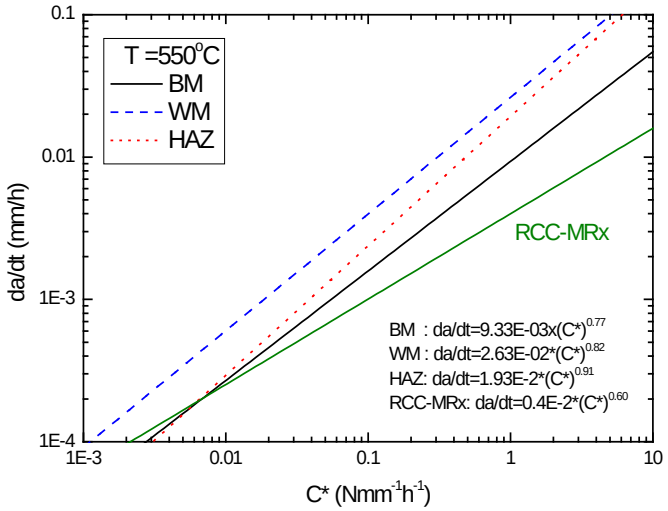

Figure 5. Comparison of CCGR curves for the BM, WM, and HAZ

Construction of CCGR Equations

Figure 4 shows the plots of C^* vs. da/dt obtained for the BM, WM, and HAZ of Gr. 91 steel at 550°C. The solid lines show the regression curves obtained using the least squares fit method for each CCG data. The creep crack growth laws for the BM, WM, and HAZ were defined, as follows:

$$da/dt = 9.33 \times 10^{-3} (C^*)^{0.77} \quad \text{(for BM)} \tag{9}$$
(validity range : $0.05 < C^* < 3.05$ N/mm.h)

$$da/dt = 2.63 \times 10^{-2} (C^*)^{0.82} \quad \text{(for WM)} \tag{10}$$
(validity range : $0.013 < C^* < 0.60$ N/mm.h)

$$da/dt = 1.93 \times 10^{-2} (C^*)^{0.91} \quad \text{(for HAZ)} \tag{11}$$
(validity range : $0.02 < C^* < 3.27$ N/mm.h)

When the three CCGR curves for the BM, WM, and HAZ were overlapped together, as shown in Figure 4, it appears clearly that the WM and HAZ are faster than BM. The WM is about 2.8 times faster than the BM. The CCGR line of the HAZ is transitionally changed and positioned between the WM and BM. The HAZ is thought to be complex with the inhomogeneity among those materials affects the state of stress field or strain rate field near the weld fusion line and near the BM/HAZ interface, as a transition region between the BM and WM. It is assumed that the CCGR in the creep crack growth tests was similar to the creep strain rate in the creep tests.
In addition, the CCGR law of the BM obtained in the present investigation was compared with currently elevated temperature design (ETD) code in French, the RCC-MRx (Afcen (2015)), as shown in Figure 5. As seen well in the figure, the RCC-MRx is more conservative in the CCGR line than the KAERI tested data obtained in the present investigation. For the result, to more clearly define the CCGR law of Gr. 91 steel, a number of data will be required for a design use, and also the CCG database will be needed to be established through a large body of CCG tests because the CCG behavior will be different due to various experimental conditions: specimen sizes, material conditions, test methods, and environments, etc.

CONCLUSIONS

To evaluate the CCGR for the BM, WM, and HAZ of Gr. 91 weldments, a series of creep and creep crack growth tests were carried out under different applied loads at 550°C. Creep crack growth laws for the BM, WM, and HAZ were constructed using the empirical equation of da/dt vs. the C^* parameter and compared. Results showed that the WM and HAZ were faster than BM, and the WM was found to be about 2.8 times faster in the CCGR than the BM. The CCGR line of the HAZ was positioned between the WM and BM. The reason for this was that the HAZ was inhomogeneity as a transition region between the BM and WM. It was assumed that the CCGR in the creep crack growth tests was similar behavior to the creep strain rate in the creep tests. The RCC-MRx was found to be more conservative in the CCGR than the KAERI tested data obtained in the present investigation.

ACKNOWLEDGEMENTS

This work was supported by the National Research Foundation of Korea (NRF) grant funded by the Korea government (MSIP) (No. 2017M2A8A1014758).

REFERENCES

Afcen RCC-MRx (2015). *Code Section III – Tome 6, Probationary Phase Rules*, France.

ASTM E139-13 (2013). *Standard Test Method for Conducting Creep, Creep-Rupture and Stress Rupture Tests of Metallic Materials*, USA.

ASTM E1457-13 (2013). *Standard Test Method for Measurement of Creep Crack Growth Rates in Metals*, USA.

Choudhary, B.K., Bhanu Sankara Rao, K. and Mannan, S.L. (1999). "Steady state creep deformation behavior of 9Cr-1Mo ferritic steel forging in quenched and tempered condition," *Trans. Indian Inst. Met.*, 52 327-336.

Dogan, B. and Petrovski, B. (2001). "Creep crack growth of high temperature weldments," *Int J Press Vessels Piping*, 78 795-805.

Kim, W.G., Park, J.Y., Hong, S.D. and Kim, S.J.(2011), "Probabilistic assessment of creep crack growth rate for Gr. 91 steel," *Nuclear Engineering and Design*, 241, 3580-3586.

Kim, W.G., Park, J.Y., Lee, H.Y., Hong, S.D., Kim, Y.Y. and Kim, S.J. (2013), "Time-dependent crack growth behavior for a SMAW weldment of Gr. 91 steel," *Int J Press Vessels Piping*, 110, 66–71.

Nikbin, K.M., Smith, D.J. and Webster, G.A. (1986). "An Engineering approach to the prediction of creep crack growth," *Transactions of the ASME*, 108 186-191.

Saxena, A. (1997). *Nonlinear Fracture Mechanics for Engineers*, CRC Press, New York, USA.

Sugiura, R., Yokobori, J., Tabuchi, M. and Yokobori, T. (2007). "Comparison of creep crack growth rate in heat affected zone of welded joint for 9% Cr ferritic heat resistance steel based on C*, dδ/dt, K and Q* parameter," *Engineering Fracture Mechanics*, 74 868-881.

Takahasi,Y., Igari,T., Kawashima, F., Date, S., Isobe, N., Itoh, T., Noguchi, Y. and Kobayashi, K. (2005). "High-Temperature Crack Growth Behavior of High-Chromium Steels," *SMiRT 18*, SMiRT18-G11-7 1904-1915.

Tabuchi, M., Watanabe, T., Kubo, K., Matsui, M., Kinugawa, J. and Abe, F. (2001). "Creep crack growth behavior in the HAZ of weldments of W containing high Cr steel," *Int J Press Vessels Piping*, 78, 779–784.

Yamamoto, M., Miura, N. and Ogata, T. (2010), "Applicability of C^* parameter in assessing Type–IV creep cracking in mod. 9Cr-1Mo steel welded joint," *Engineering Fracture Mechanics*, 77 3022-3034.